Biochemical and Biophysical Research Communications 440 (2013) 737–742

Contents lists available at ScienceDirect

Biochemical and Biophysical Research Communications

journal homepage: www.elsevier.com/locate/ybbrc

Nucleoredoxin regulates glucose metabolism via phosphofructokinase 1

Yosuke Funato [a,1], Tatsuya Hayashi [a,1], Yasuhiro Irino [b], Tadaomi Takenawa [b], Hiroaki Miki [a,*]

[a] Department of Cellular Regulation, Research Institute for Microbial Diseases, Osaka University, Suita, Osaka 565-0871, Japan
[b] Integrated Center for Mass Spectrometry, Kobe University Graduate School of Medicine, Kobe 650-0017, Japan

ARTICLE INFO

Article history:
Received 24 September 2013
Available online 8 October 2013

Keywords:
Glycolysis
Pentose phosphate pathway
Oxidative stress
Antioxidants
Phosphofructokinase 1
Nucleoredoxin

ABSTRACT

Phosphofructokinase (PFK) 1 is a glycolytic enzyme, and its abnormality contributes to the development of multiple human diseases, such as cancer. Here, we report that nucleoredoxin (NRX), a thioredoxin-related oxidoreductase, is a novel interacting partner of PFK1. NRX binds directly to PFK1, and endogenous NRX and PFK1 interact *in vivo*. In $NRX^{-/-}$ mouse embryonic fibroblasts (MEFs), the oligomerization status of PFK1 is altered and the catalytic activity of PFK1 is decreased. *NRX* deficiency augmented levels of NADPH and reduced glutathione, two major cellular antioxidants generated through the pentose phosphate pathway. Indeed, $NRX^{-/-}$ MEFs are significantly more resistant to oxidative stress than $NRX^{+/+}$ MEFs. These results reveal a novel role of NRX in the regulation of PFK1 activity and in the balance between glycolysis and the pentose phosphate pathway.

1. Introduction

Glucose metabolism is a fundamental aspect of cell physiology. PFK1 is a glycolytic enzyme that phosphorylates fructose-6-phosphate (F6P), forming fructose-1,6-bisphosphate (F1,6BP) [1]. This reaction is virtually irreversible under normal intracellular conditions and has been considered as the important regulatory step in glycolysis. There are multiple mechanisms regulating the activity of PFK1, which are modulated by a variety of metabolites and proteins. It is well known that PFK1 activity is strongly inhibited by ATP, whereas AMP, the dephosphorylated form of ATP, counteract the inhibitory effect of ATP on PFK1 [2]. Such regulations of PFK1 by cellular metabolites are considered to fine-tune the glycolytic rate to meet the energy demands of the cell.

Since the discovery of aerobic glycolysis in cancer cells, the so-called "Warburg effect" [3], a great deal of attention has been focused on the relationship between glucose metabolism and human cancers [4]. Recent studies have revealed a concrete molecular link between PFK1 and cancer-related molecules. Bensaad et al. reported that the tumor-suppressor protein p53 induces the expression of TP53-induced glycolysis and apoptosis regulator (TIGAR), a phosphatase that degrades fructose-2,6-bisphosphate (F2,6BP) [5]. F2,6BP is a potent positive allosteric activator of PFK1, which counteracts the inhibitory effect of ATP, and thus p53 can suppress PFK1 activity, by lowering levels of F2,6BP through TIGAR expression. Recently, another regulatory mechanism involving glycosylation of PFK1 itself was reported [6]. Yi et al. discovered that covalent addition of *N*-acetylglucosamine to PFK1 inhibits its activity and shifts the glucose metabolism toward the pentose phosphate pathway (PPP), which confers a growth advantage to cancer cells. Taken together, PFK1 appears to be one of the key enzymes regulating the global metabolic state of cells, of which abnormality contributes to the development of multiple human diseases such as cancer.

NRX is a thioredoxin (TRX)-related oxidoreductase that can reduce disulfide bonds in insulin using an *in vitro* experimental assay [7]. TRX family proteins commonly possess a pair of redox-active cysteine (Cys) residues in the catalytic center, which are sensitive to oxidation and directly involved in the reduction of disulfide bonds in target proteins [8]. In the case of TRX, many oxidoreductase substrates have been characterized and its importance in maintaining the normal intracellular redox status is well established. In contrast, previous studies have shown that NRX directly binds and stabilizes dishevelled, an essential component in Wnt signaling, and inhibits its signaling function [9,10]. In addition, NRX also functions as an adaptor linking flightless-I and myeloid differentiation primary response gene (88), and negatively regulates the activity of toll-like receptor 4-mediated innate im-

Abbreviations: PFK, phosphofructokinase; NRX, nucleoredoxin; MEFs, mouse embryonic fibroblasts; F6P, fructose-6-phosphate; F1,6BP, fructose-1,6-bisphosphate; TIGAR, TP53-induced glycolysis and apoptosis regulator; F2,6BP, fructose-2,6-bisphosphate; PPP, pentose phosphate pathway; TRX, thioredoxin; Cys, cysteine; MBP, maltose-binding protein; H_2O_2, hydrogen peroxide; GSH, reduced glutathione.

* Corresponding author. Address: Department of Cellular Regulation, Research Institute for Microbial Diseases, Osaka University, 3-1 Yamadaoka, Suita, Osaka 565-0871, Japan. Fax: +81 6 6879 8295.
E-mail address: hmiki@biken.osaka-u.ac.jp (H. Miki).

[1] These authors contributed equally to this work.

0006-291X/$ - see front matter © 2013 Elsevier Inc. All rights reserved.
http://dx.doi.org/10.1016/j.bbrc.2013.09.138

mune response elicited by lipopolysaccharide [11]. Thus, NRX is considered to be a multifunctional protein [12].

In this study, we report that NRX interacts with PFK1 and maintains its activity. Also, *NRX*-deficient cells possess elevated levels of PPP-derived antioxidants, thereby enhancing cellular resistance to oxidative stress.

2. Materials and methods

2.1. Expression constructs

Mouse PFK1 cDNAs [platelet (P), muscle (M), and liver (L) forms] were purchased from Invitrogen (IMAGE clones 2655383 and 3495173 for P and M forms, respectively) and ORIGENE (MC203910 for the L form). Mouse NRX cDNAs (WT and Mut) were generated as described previously [9]. PFK1 and NRX cDNAs were inserted into appropriate expression vectors (pEF–BOS, pCMV, pFastBac, pMAL, or pQE) for use.

2.2. Antibodies

Anti-NRX rabbit polyclonal antibody was generated in a previous study [9]. The following commercially available antibodies were also used; mouse monoclonal antibodies against FLAG (SIGMA), and rabbit polyclonal antibodies against PFK1 (Bioworld Technology), FLAG (SIGMA), and Myc (Santa Cruz).

2.3. Cell culture

HEK293 cells were cultured in DMEM supplemented with 10% fetal bovine serum and antibiotics. Expression plasmids were transfected using Lipofectamine2000 (Invitrogen). Primary MEFs were isolated from $NRX^{+/+}$ or $NRX^{-/-}$ mice from a C57BL/6J background and cultured according to standard methods as reported previously [10]. Plasmids were transfected into MEFs using the Neon™ transfection system (Invitrogen). Cell culture under hypoxic conditions was performed using a multi-gas incubator (MCO-5M; SANYO).

2.4. Identification of NRX-interacting proteins by mass spectrometry

Recombinant GST or GST-NRX proteins were expressed in Sf9 insect cells and immobilized on glutathione–sepharose beads (GE Healthcare). The beads were mixed with mouse testis lysates. Bound proteins were separated by SDS–PAGE, followed by silver staining using a SilverQuest™ kit (Invitrogen). Bands of interest were excised from the gel and trypsin-digested peptides were subjected to mass spectrometry as described previously [9].

2.5. Recombinant proteins

His-NRX proteins were expressed in *Escherichia coli* and purified using Ni–NTA beads (QIAGEN). The purified proteins were eluted with imidazole and used immediately for assays. Maltose-binding protein (MBP) and MBP–PFK1 (P form) were also expressed in *E. coli*, purified with amylose resin (New England Biolabs), and the purified proteins on the resin were subjected to pull-down assays.

2.6. Immunoprecipitation

Immunoprecipitation experiments with anti-FLAG antibody were performed using standard methods described previously [13]. For immunoprecipitation with anti-NRX antibody, we used a modified method to covalently attach the antibody to the beads, as the IgG heavy chain migrates just above endogenous NRX in SDS–PAGE and it was difficult to detect the NRX signal. Briefly, we covalently cross-linked the antibody and protein A-agarose beads by incubating them with 20 mM dimethylpimelimidate (Sigma) for 30 min at room temperature, and then the beads were mixed with MEF lysates.

2.7. Assessment of cell viability

Cell viability was determined by Trypan blue exclusion method as described previously [14], with slight modifications. Cells (2×10^5/dish) were seeded in 36-mm dishes the day prior to analyses. After treatment with 1 mM hydrogen peroxide (H_2O_2) for the indicated times, detached cells were collected and the remaining adherent cells were collected by trypsinization. Both cell fractions were combined and centrifuged. Cell pellets were resuspended in PBS, and then mixed with 0.4% Trypan blue solution (Invitrogen). Cells without blue staining were determined to be viable.

2.8. Measurement of PFK1 activity

PFK1 catalytic activity was measured by the consumption of NADH in a reaction mixture, according to a method described previously [15]. Briefly, cell lysates (10 μg total protein) were mixed with reaction buffer (50 mM HEPES [pH 7.0], 100 mM KCl, 5 mM $MgCl_2$, 1.5 mM ATP, 0.15 mM NADH, 5 mM Na_2HPO_4, 0.1 mM AMP, 1 mM NH_4Cl, 5 units/mL of triosephosphate isomerase, 0.5 units/mL of aldolase, 0.5 units/mL of glycerophosphate dehydrogenase, and 5 mM of F6P). The mixture was incubated at room temperature, and the absorbance at 340 nm, which reflects the amount of NADH, was determined for a period of 15–20 min.

2.9. Measurement of ATP and reduced glutathione (GSH) levels, and determination of the NADPH/$NADP^+$ ratio

Intracellular ATP and GSH levels were measured with the CellTiter-Glo Luminescent Cell Viability Assay kit (Promega) and BIOXYTECH GSH-400 kit (OxisResearch), respectively, according to the manufacturers' instructions. NADPH/$NADP^+$ ratios were determined by using $NADP^+$/NADPH Quantification Kit (BioVision), which utilizes an enzyme-based colorimetric reaction.

2.10. Native PAGE

Native PAGE was performed as previously described [16], with minor modifications. Cell lysates were mixed with 4× sample buffer for native PAGE (40% glycerol, 0.4% BPB, 0.2 M Tris–HCl [pH 6.8], and 40 mM iodoacetoamide) and subjected to native PAGE analyses. The cathode and anode buffer were as follows: cathode buffer; 25 mM Tris–HCl (pH 8.4), 192 mM glycine, 0.1% deoxycholate; anode buffer; 25 mM Tris–HCl (pH 8.4), 192 mM glycine.

2.11. Statistics

All statistical data are presented as means ± SEM. p Values were obtained using a Student's two-tailed t-test.

3. Results

3.1. Identification of PFK1 as an NRX-interacting protein

To search for novel NRX-interacting protein(s), we performed pull-down assays using the GST–NRX fusion proteins as bait. We

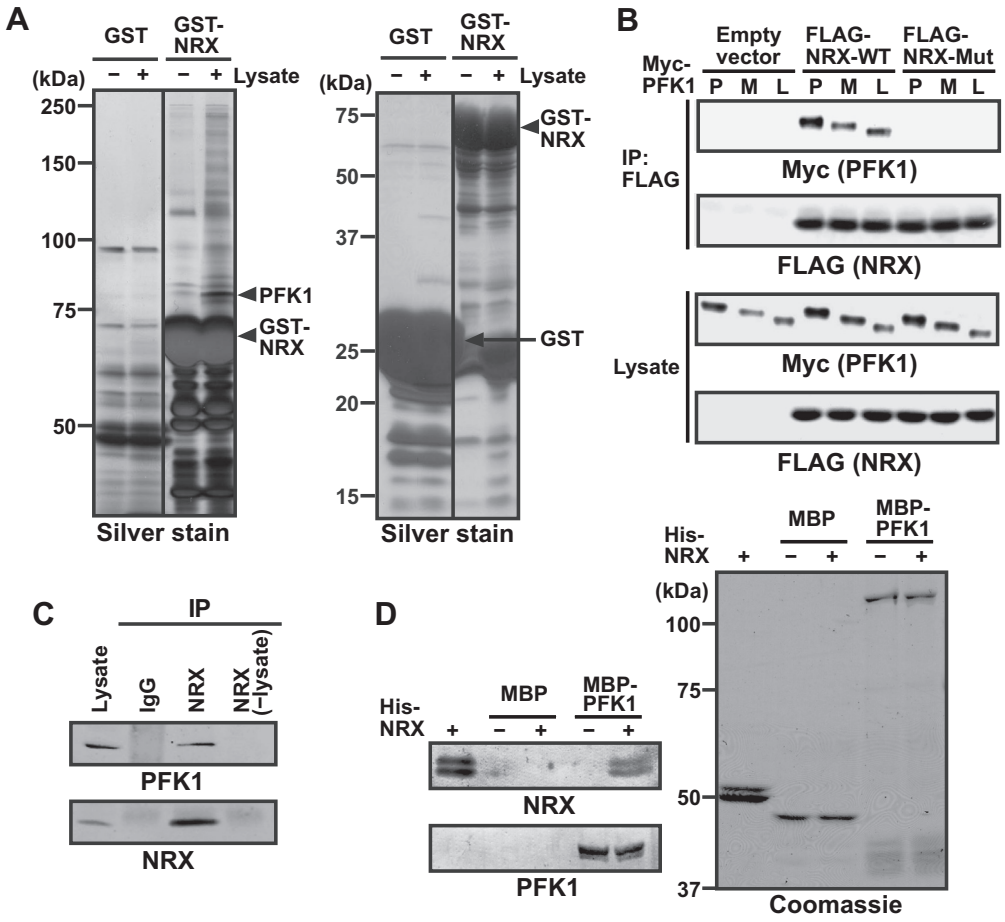

Fig. 1. Identification of PFK1 as an NRX-interacting protein. (A) Mouse testis lysates were mixed with GST or GST–NRX immobilized on glutathione-sepharose beads. Bound proteins were subjected to SDS–PAGE and visualized by silver staining. Arrowheads indicate GST–NRX or PFK1, and an arrow indicates GST. (B) The indicated expression constructs were transfected into HEK293 cells (P: platelet form, M: muscle form, L: liver form). Cell lysates were immunoprecipitated with anti-FLAG antibody, followed by immunoblotting with the indicated antibodies. (C) MEF lysates were subjected to immunoprecipitation with an anti-NRX antibody. The precipitates were separated by SDS–PAGE, followed by immunoblotting with an anti-PFK1 antibody and (D) MBP or MBP–PFK1 (P form) was immobilized on beads and then mixed with His-NRX proteins. The bound proteins were subjected to SDS–PAGE, followed by immunoblotting with the indicated antibodies (left panel). His-NRX, MBP, and MBP–PFK1 protein purity, as determined by Coomassie staining, is also shown (right panel).

used mouse testis lysates as the source material, as NRX is most abundantly expressed in the testis of adult mice [7]. As shown in Fig. 1A, several proteins were specifically precipitated by GST–NRX. Among them, the most abundant protein band at approximately 80-kDa was subjected to mass spectrometry and identified to be PFK1. Three isoforms of PFK1, which are encoded by different genes, are known; P, M, and L forms. We co-expressed each of these PFK1 isoforms with NRX in cells and performed co-immunoprecipitation analyses to investigate their interaction. The results indicated that wild-type NRX (NRX–WT) bound similarly to all three PFK1 isoforms (Fig. 1B). We also performed similar experiments using NRX–Mut, a mutant form of NRX that lacks two Cys residues (Cys205 and Cys208) essential for oxidoreductase activity, and found that it did not bind to PFK1. We next investigated the complex formation of endogenous proteins. Cell lysates were subjected to immunoprecipitation with an anti-NRX antibody, and the resulting precipitates were analyzed by immunoblotting with an anti-PFK1 antibody. A clear co-precipitation was observed, whereas negative control experiments using rabbit IgG or without lysates yielded no positive signals (Fig. 1C). To examine whether the interaction was direct, we performed *in vitro* binding assays using purified recombinant proteins of His-NRX and MBP–PFK1 proteins. As shown in Fig. 1D, a weak but significant positive signal was observed when we subjected His-NRX proteins to pull-down assays with MBP–PFK1.

3.2. Decreased PFK1 activity in $NRX^{-/-}$ MEFs

We next investigated whether NRX affects the enzymatic activity of PFK1. For this purpose, we used MEFs isolated from wild-type ($NRX^{+/+}$) or *NRX*-deficient ($NRX^{-/-}$) mice, generated in our previous study [11]. We prepared MEF lysates and subjected them to an enzyme assay for PFK1, designed to indicate the reaction progress via decreased NADH levels (Fig. 2A). Indeed, NADH levels were rapidly decreased by the addition of $NRX^{+/+}$ MEF lysates to the reaction mixture, whereas the negative control sample (without lysate) showed no significant change. In addition, the decreased NADH was mostly inhibited by the addition of 10 mM ATP, a potent allosteric inhibitor of PFK1 [2]. We then compared PFK1 activity of $NRX^{+/+}$ and $NRX^{-/-}$ MEF lysates (both transfected with control GFP) and found that the latter also had decreased NADH but the speed of the decrease was slightly slower than in the former (Fig. 2B and C). To confirm that this difference was due to the absence of endogenous NRX, we transfected $NRX^{-/-}$ MEFs with expression constructs of either NRX–WT or NRX–Mut. As indicated in the same panels, expression of NRX–WT, but not of NRX–Mut, restored PFK1 activity to normal levels. Taken together, these results indicate that endogenous NRX sustains PFK1 activity in cells.

PFK1 catalyzes an essential step in the glycolytic pathway, and thus changes in PFK1 activity presumably affect the cellular metabolic state. We quantified ATP levels in $NRX^{+/+}$ and $NRX^{-/-}$ MEFs,

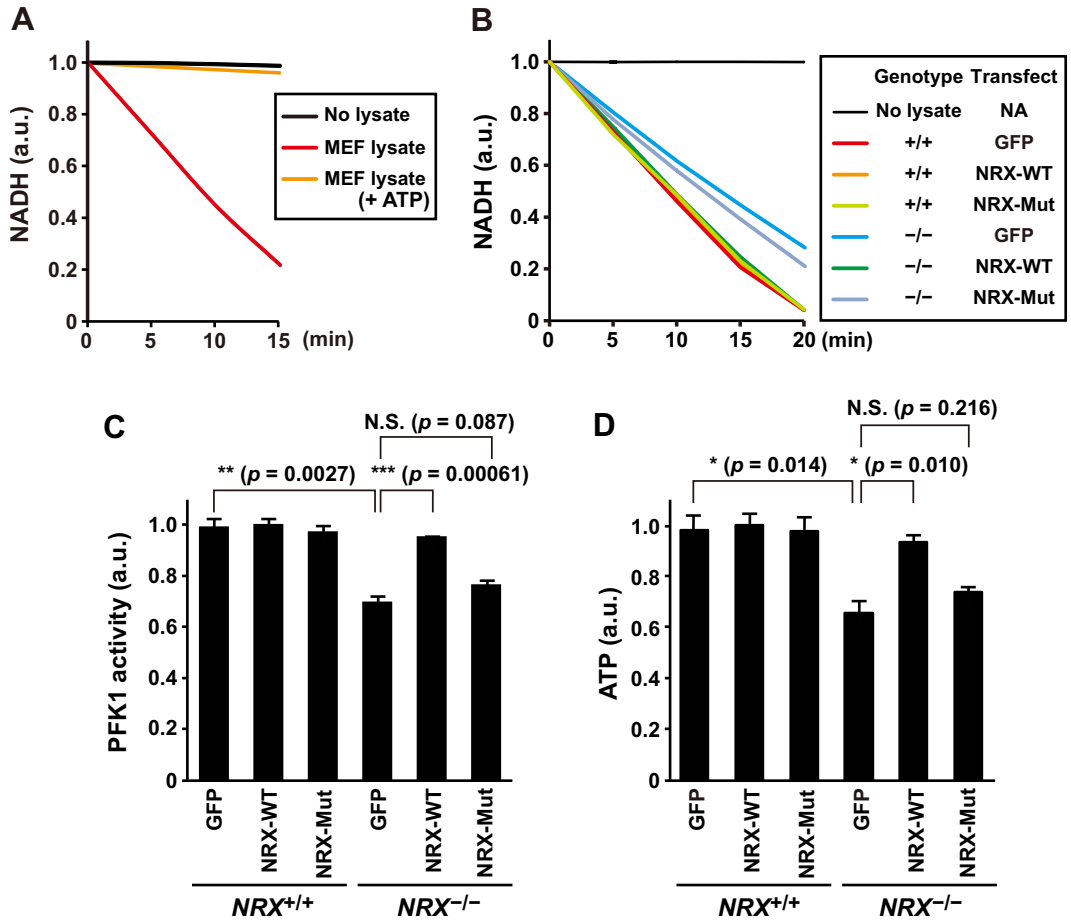

Fig. 2. Decreased PFK1 activity in $NRX^{-/-}$ MEFs. (A) $NRX^{+/+}$ MEF lysates were analyzed for PFK1 activity by measuring NADH consumption. "+ATP" indicates that the reaction mixture includes 10 mM ATP. (B) Lysates of $NRX^{+/+}$ or $NRX^{-/-}$ MEFs transfected with the indicated constructs were analyzed for PFK1 activity by measuring NADH consumption. (C) Relative PFK1 activities were determined by the amount of consumed NADH at 15 min after the start of the reaction. The data are shown as mean ± SEM ($n = 3$). p Values were determined by Student's two-tailed t-test (paired). $^{**}p < 0.01$, $^{***}p < 0.001$, N.S.: not significant and (D) ATP levels of $NRX^{+/+}$ or $NRX^{-/-}$ MEFs transfected with the indicated constructs were determined. The data are shown as means ± SEM ($n = 3$). p Values were determined by Student's two-tailed t-test (paired). $^{*}p < 0.05$, N.S.: not significant.

and found that levels in $NRX^{-/-}$ MEFs were significantly decreased and the expression of NRX–WT again restored it to normal levels (Fig. 2D), consistent with the role of NRX in the regulation of cellular metabolism via modulation of PFK1 activity.

3.3. Altered PFK1 oligomerization status by NRX

It has been shown that the oligomerization status of PFK1 is linked to its enzymatic activity [17,18]. In addition, a recent report showed that complex formation between ectopically expressed FLAG–PFK1 and endogenous PFK1 correlates with PFK1 oligomerization status [6]. Therefore, we performed co-immunoprecipitation experiments with $NRX^{+/+}$ and $NRX^{-/-}$ MEF lysates transfected with FLAG–PFK1. As shown in Fig. 3A, co-precipitation levels of endogenous PFK1 in the anti-FLAG immunoprecipitates were decreased in $NRX^{-/-}$ MEFs. This decrease is due to the absence of endogenous NRX, because co-expression of NRX–WT, but not NRX–Mut, restored complex formation to normal levels.

We next directly investigated the oligomerization status of PFK1. Here, lysates of MEFs transfected with FLAG–PFK1 were subjected to PAGE under native conditions. Yi and colleagues reported that cell culture under hypoxic conditions, which induces PFK1-glycosylation and downregulation of its catalytic activity, resulted in the appearance of a faster migrating band [6]. Consistently, we also observed a similar faster migrating band of FLAG–PFK1 when cells were subjected to hypoxic conditions (Fig. 3B). This faster migrating band was also observed in the lane with $NRX^{-/-}$ MEF lysates, and disappeared upon NRX co-expression. Collectively, these results implicate NRX in regulation of the oligomerization status of PFK1, which likely affects its catalytic activity.

3.4. Augmentation of antioxidant levels in $NRX^{-/-}$ MEFs

PFK1 phosphorylates F6P and converts it to F1,6BP. Thus, partial inhibition of the PFK1 activity can redirect glucose metabolism to the PPP, which emanates from glucose-6-phosphate existing in a chemical equilibrium with F6P. One of the primary products of the PPP is NADPH, which is used in cells to prevent oxidative stress. Therefore, we determined the ratio of NADPH (reduced form) to $NADP^+$ (oxidized form) with an enzyme-based colorimetric method, and expectedly, the ratio of NADPH/$NADP^+$ was estimated to be roughly doubled in $NRX^{-/-}$ MEFs (Fig. 4A). Moreover, this increase was suppressed by expressing NRX–WT, indicating that endogenous NRX suppresses NADPH levels. NADPH contributes to the regeneration of the reduced form of GSH, one of major antioxidants in cells, by donating electrons via glutathione reductase. Thus, we also investigated GSH levels in $NRX^{+/+}$ and $NRX^{-/-}$ MEFs, and the results were very similar to those of NADPH (Fig. 4B).

As we confirmed an increase in the major intracellular antioxidants, NADPH and GSH, in $NRX^{-/-}$ MEFs, we investigated

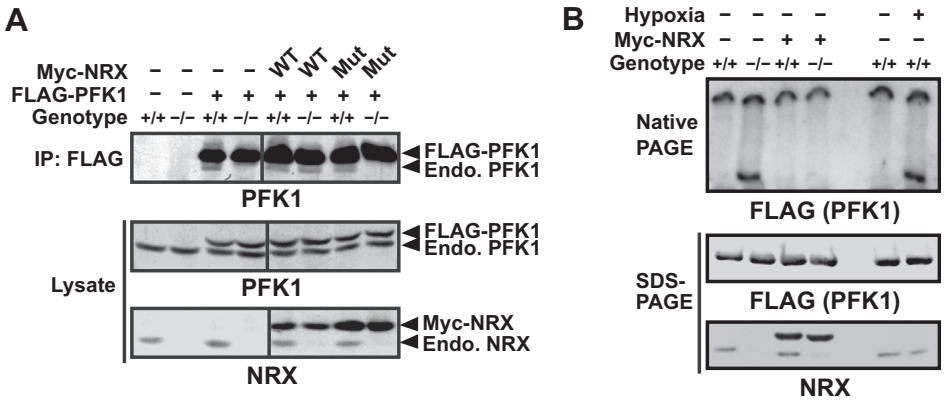

Fig. 3. Oligomerization status of PFK1. (A) Lysates of *NRX*$^{+/+}$ or *NRX*$^{-/-}$ MEFs transfected with FLAG–PFK1 (P form) and the indicated Myc-NRX constructs (WT or Mut) were subjected to anti-FLAG immunoprecipitation. The precipitates were separated by SDS–PAGE, followed by immunoblotting with the indicated antibodies. (B) Lysates of *NRX*$^{+/+}$ or *NRX*$^{-/-}$ MEFs transfected with the indicated constructs were subjected to immunoblotting under native or standard denaturing conditions. The P form of FLAG–PFK1 was used. Cell culture under hypoxic conditions was conducted with 1% O_2 for 24 h.

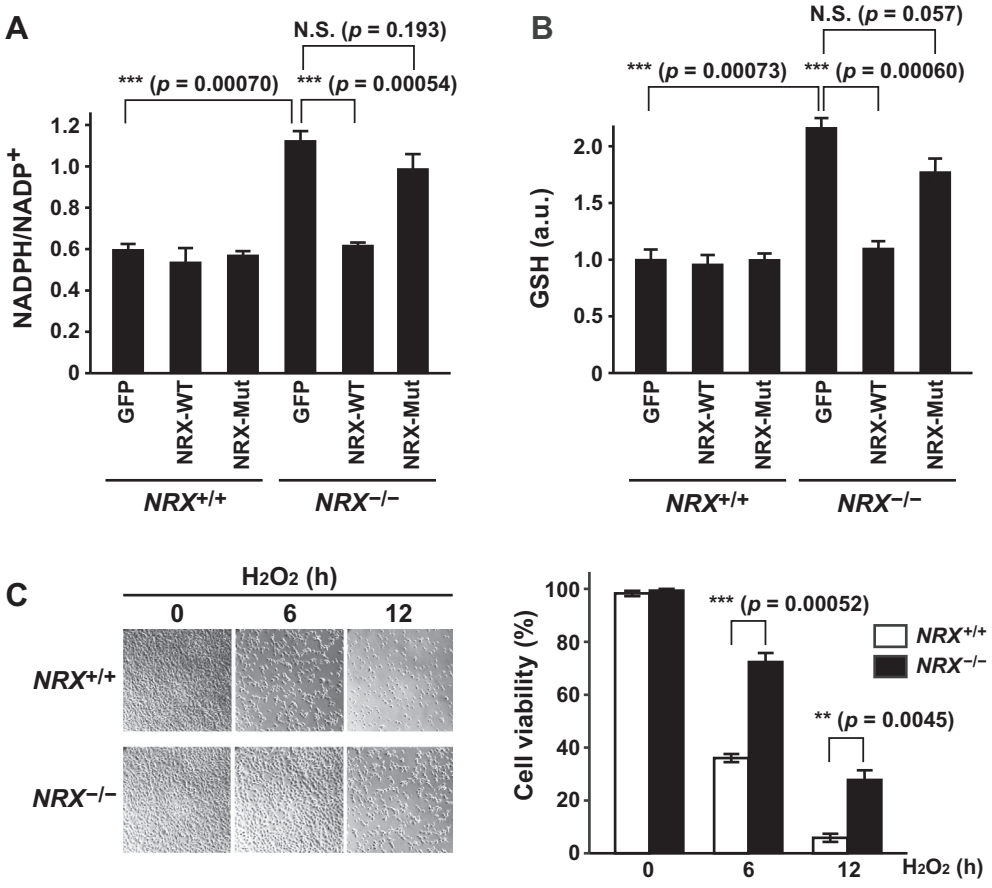

Fig. 4. Increased antioxidant levels in *NRX*$^{-/-}$ MEFs. (A) NADPH/NADP$^+$ ratios in *NRX*$^{+/+}$ or *NRX*$^{-/-}$ MEFs transfected with the indicated constructs were determined. The data are shown as means ± SEM ($n = 3$). p Values were determined by Student's two-tailed t-test (paired). $^{***}p < 0.001$, N.S.: not significant. (B) GSH levels of *NRX*$^{+/+}$ or *NRX*$^{-/-}$ MEFs transfected with the indicated constructs were determined. The data are shown as means ± SEM ($n = 3$). p Values were determined by Student's two-tailed t-test (paired). $^{***}p < 0.001$, N.S.: not significant and (C) *NRX*$^{+/+}$ or *NRX*$^{-/-}$ MEFs were treated with 1 mM H_2O_2 for the indicated times. Representative images of the cells on culture dishes are shown. The graph data shows percentages of cell viability, as determined by Trypan blue exclusion test (means ± SEM, $n = 3$). p Values were determined by Student's two-tailed t-test (paired). $^{**}p < 0.01$, $^{***}p < 0.001$.

the resistance of cells to oxidative stress. *NRX*$^{+/+}$ and *NRX*$^{-/-}$ MEFs were treated with a toxic level of H_2O_2 (1 mM), and then, the cell morphology was observed. As shown in Fig. 4C (left panel), *NRX*$^{+/+}$ MEFs became mostly detached from the culture dish 12 h after treatment. For *NRX*$^{-/-}$ MEFs, cell detachment was also observed, but a larger number of cells remained attached. To quantitatively assess the cellular damage, we examined the viability of cells (both attached and detached) by Trypan blue exclusion. The results clearly confirmed that *NRX*$^{-/-}$ MEFs were significantly more resistant to oxidative stress than *NRX*$^{+/+}$ MEFs (Fig. 4C, right panel).

4. Discussion

In this study, we identified a novel role of NRX, as a regulator of PFK1 oligomerization and catalytic activity. PFK1 activity was decreased in *NRX*$^{-/-}$ MEFs (Fig. 2), which would shift glucose metabolism to the PPP and thus make cells more resistant to oxidative stress (Fig. 4). However, the mechanism of how NRX affects PFK1 oligomerization remains unclear. The higher mobility form of PFK1 oligomer was observed in lysates from both *NRX*$^{-/-}$ MEFs and hypoxia-treated MEFs (Fig. 3). It was recently reported that hypoxia induces the covalent addition of *N*-acetylglucosamine to PFK1, resulting in the downregulation of its catalytic activity [6]. Thus, we speculated that hyperglycosylation of PFK1 may occur in *NRX*$^{-/-}$ MEFs, which could explain the appearance of the higher mobility form of PFK1 and its decreased enzymatic activity. We performed immunoblotting analyses with an antibody that recognizes both free and protein-linked forms of *N*-acetylglucosamine, but failed to detect any significant PFK1 hyperglycosylation in *NRX*$^{-/-}$ MEFs (data not shown). Apart from glycosylation, PFK1 is also subject to phosphorylation [19] and acylation [20]. More comprehensive analyses would be required to reveal the presence and the identity of PFK1 modification(s), affected by NRX deficiency, and to clarify the molecular mechanism of PFK1 regulation by NRX.

The PPP supplies cells with antioxidants and nucleosides, and thus is important in promoting cell proliferation and tumor growth [21]. Indeed, it was recently reported that disruption of *TIGAR*, the gene for the abovementioned F2,6BP phosphatase which stimulates PPP, decreased tumor burden in a mouse model of intestinal adenoma [22]. Furthermore, using an *in vitro* organoid culture model, the authors showed that impaired growth of *TIGAR*$^{-/-}$ cells derived from the crypt of the small intestine was rescued by supplementation with nucleosides and the antioxidant *N*-acetyl cysteine. Since *NRX*$^{-/-}$ mice are perinatally lethal [10], it is impossible to perform such kinds of experiments using *NRX*$^{-/-}$ mice. However, it should be noted that RNAi knockdown of NRX promoted cancerous transformation in NIH3T3 cells expressing oncogenic Ras [9]. We originally concluded that this augmentation in cellular transformation was achieved through aberrant activation of Wnt signaling, as NRX directly binds to dishevelled and inhibits its signaling in the Wnt pathway. Based on our findings in this study, PPP activation in the absence of endogenous NRX may also contribute to the malignant growth of these cells. Future studies including experiments using NRX conditional knockout mice will gain more insights into the role of NRX in tumorigenesis *in vivo*.

Role of funding sources

This work was supported by Funding Program for Next Generation World-Leading Researchers from Japan Society for the Promotion of Science (JSPS) to H.M., Exciting Leading-Edge Research Projects from Osaka University to H.M., and Grants-in-Aid for Scientific Research from JSPS and Ministry of Education, Culture, Sports, Science and Technology-Japan to H.M. and Y.F.

Acknowledgments

We thank M. Okada and K. Saito for mass spectrometry analyses, and H. Yamamoto for technical supports.

References

[1] I. Mor, E.C. Cheung, K.H. Vousden, Control of glycolysis through regulation of PFK1: old friends and recent additions, Cold Spring Harb. Symp. Quant. Biol. 76 (2011) 211–216.
[2] J.V. Passonneau, O.H. Lowry, Phosphofructokinase and the Pasteur effect, Biochem. Biophys. Res. Commun. 7 (1962) 10–15.
[3] O. Warburg, K. Posener, E. Negelein, Über den Stoffwechsel der Carcinomzelle, Biochem. Zeitschr. 152 (1924) 309–344.
[4] W.H. Koppenol, P.L. Bounds, C.V. Dang, Otto Warburg's contributions to current concepts of cancer metabolism, Nat. Rev. Cancer 11 (2011) 325–337.
[5] K. Bensaad, A. Tsuruta, M.A. Selak, M.N. Vidal, K. Nakano, R. Bartrons, E. Gottlieb, K.H. Vousden, TIGAR, a p53-inducible regulator of glycolysis and apoptosis, Cell 126 (2006) 107–120.
[6] W. Yi, P.M. Clark, D.E. Mason, M.C. Keenan, C. Hill, W.A. Goddard 3rd, E.C. Peters, E.M. Driggers, L.C. Hsieh-Wilson, Phosphofructokinase 1 glycosylation regulates cell growth and metabolism, Science 337 (2012) 975–980.
[7] H. Kurooka, K. Kato, S. Minoguchi, Y. Takahashi, J. Ikeda, S. Habu, N. Osawa, A.M. Buchberg, K. Moriwaki, H. Shisa, T. Honjo, Cloning and characterization of the nucleoredoxin gene that encodes a novel nuclear protein related to thioredoxin, Genomics 39 (1997) 331–339.
[8] C.H. Lillig, A. Holmgren, Thioredoxin and related molecules – from biology to health and disease, Antioxid. Redox Signal. 9 (2007) 25–47.
[9] Y. Funato, T. Michiue, M. Asashima, H. Miki, The thioredoxin-related redox-regulating protein nucleoredoxin inhibits Wnt–beta-catenin signalling through dishevelled, Nat. Cell Biol. 8 (2006) 501–508.
[10] Y. Funato, T. Terabayashi, R. Sakamoto, D. Okuzaki, H. Ichise, H. Nojima, N. Yoshida, H. Miki, Nucleoredoxin sustains Wnt/β-catenin signaling by retaining a pool of inactive dishevelled protein, Curr. Biol. 20 (2010) 1945–1952.
[11] T. Hayashi, Y. Funato, T. Terabayashi, A. Morinaka, R. Sakamoto, H. Ichise, H. Fukuda, N. Yoshida, H. Miki, Nucleoredoxin negatively regulates Toll-like receptor 4 signaling via recruitment of flightless-I to myeloid differentiation primary response gene (88), J. Biol. Chem. 285 (2010) 18586–18593.
[12] Y. Funato, H. Miki, Nucleoredoxin, a novel thioredoxin family member involved in cell growth and differentiation, Antioxid. Redox Signal. 9 (2007) 1035–1057.
[13] T. Terabayashi, T.J. Itoh, H. Yamaguchi, Y. Yoshimura, Y. Funato, S. Ohno, H. Miki, Polarity-regulating kinase partitioning-defective 1/microtubule affinity-regulating kinase 2 negatively regulates development of dendrites on hippocampal neurons, J. Neurosci. 27 (2007) 13098–13107.
[14] M. Jazvinšćak Jembrek, L. Vuković, J. Puhović, J. Erhardt, N. Oršolić, Neuroprotective effect of quercetin against hydrogen peroxide-induced oxidative injury in P19 neurons, J. Mol. Neurosci. 47 (2012) 286–299.
[15] H. Deng, F. Yu, J. Chen, Y. Zhao, J. Xiang, A. Lin, Phosphorylation of Bad at Thr-201 by JNK1 promotes glycolysis through activation of phosphofructokinase-1, J. Biol. Chem. 283 (2008) 20754–20760.
[16] A. Morinaka, Y. Funato, K. Uesugi, H. Miki, Oligomeric peroxiredoxin-I is an essential intermediate for p53 to activate MST1 kinase and apoptosis, Oncogene 30 (2011) 4208–4218.
[17] L.K. Hesterberg, J.C. Lee, H.P. Erickson, Structural properties of an active form of rabbit muscle phosphofructokinase, J. Biol. Chem. 256 (1981) 9724–9730.
[18] M.A. Luther, G.Z. Cai, J.C. Lee, Thermodynamics of dimer and tetramer formations in rabbit muscle phosphofructokinase, Biochemistry 25 (1986) 7931–7937.
[19] I.A. Brand, H.D. Söling, Activation and inactivation of rat liver phosphofructokinase by phosphorylation–dephosphorylation, FEBS Lett. 57 (1975) 163–168.
[20] C.M. Jenkins, J. Yang, H.F. Sims, R.W. Gross, Reversible high affinity inhibition of phosphofructokinase-1 by acyl-CoA: a mechanism integrating glycolytic flux with lipid metabolism, J. Biol. Chem. 286 (2011) 11937–11950.
[21] C. Riganti, E. Gazzano, M. Polimeni, E. Aldieri, D. Ghigo, The pentose phosphate pathway: an antioxidant defense and a crossroad in tumor cell fate, Free Radic. Biol. Med. 53 (2012) 421–436.
[22] E.C. Cheung, D. Athineos, P. Lee, R.A. Ridgway, W. Lambie, C. Nixon, D. Strathdee, K. Blyth, O.J. Sansom, K.H. Vousden, TIGAR is required for efficient intestinal regeneration and tumorigenesis, Dev. Cell 25 (2013) 463–477.